ISSN 0016-7932, Geomagnetism and Aeronomy, 2014, Vol. 54, No. 3, pp. 381–387. © Pleiades Publishing, Ltd., 2014.
Original Russian Text © N.M. Gavrilov, A.V. Koval, A.I. Pogoreltsev, E.N. Savenkova, 2014, published in Geomagnetizm i Aeronomiya, 2014, Vol. 54, No. 3, pp. 412–419.

Numerical Simulation of the Influence of Stationary Mesoscale Orographic Waves on the Meridional Circulation and Ozone Fluxes in the Middle Atmosphere

N. M. Gavrilov[a], A. V. Koval[a], A. I. Pogoreltsev[b], and E. N. Savenkova[b]

[a] *St. Petersburg State University, Ul'yanovskaya ul. 3, St. Petersburg, 198504 Russia*

[b] *Russian State Hydrometeorological University, Malookhtinskii pr. 98, St. Petersburg, 195196 Russia*

e-mail: gavrilov@pobox.spbu.ru, apogor@rshu.ru

Received November 22, 2012; in final form, August 22, 2013

Abstract—The authors' parameterization of the dynamic and thermal action of stationary orographic waves generated by the Earth's surface relief is included into the model of general circulation of the middle and upper atmosphere. Numerical simulation of the general circulation in the troposphere and stratosphere was performed and the influence of stationary orographic waves propagating upward from the Earth's surface on the meridional and vertical velocity was studied. It is shown that the allowance for the dynamic and thermal action of these waves in the numerical model leads to changes by up to 20–30% in the meridional circulation and ozone fluxes associated with it at heights of the ozone layer maximum.

DOI: 10.1134/S0016793214030050

1. INTRODUCTION

In recent years, in connection with numerical simulation of the general circulation of the middle and upper atmosphere, there is increased interest in studying accelerations of the mean flow and heat influxes created by dissipating internal waves in the atmosphere. The Earth's surface topography is one important source of such waves. Orographic waves appearing as a result of the interaction between the inhomogeneous Earth's surface and inflowing atmospheric stream can propagate to the middle atmosphere and create there considerable accelerations of the mean flow and heat influxes, which can have an effect on the general circulation and thermal regime of the atmosphere. Simplified algorithms parameterizing the thermal and dynamic action of orographic waves were developed to be included into numerical models. When calculating vertical profiles of wave accelerations of the mean flow and heat influxes, the aforementioned parameterizations do not take into account the atmospheric rotation, which can have a significant effect on parameters of stationary orographic waves (SOWs) with frequencies $\sigma = 0$.

The ozone transfer between the stratosphere and troposphere has an effect on the total ozone budget in the atmosphere and on its content in the troposphere (Danielsen and Mohnen, 1977; Fishman and Crutzen, 1978). According to the present-day understanding, the main mechanism of the global ozone transfer between the troposphere and stratosphere is the ozone rise in low latitudes and ozone sink in middle and high latitudes, which is created by the general circulation of the atmosphere (Holton et al., 1995; Holton, 2002). The dynamic and thermal action of wave motions can change the general circulation of the atmosphere and thus have an effect on the global ozone transfer.

Gavrilov and Koval (2013) developed a parameterization of heat influxes and accelerations of the mean flow of SOWs that are generated upon flowing around the Earth's surface by ground streams and are then propagated into the middle atmosphere. Gavrilov et al. (2013a,b) used the aforesaid parameterization for the numerical study of changes caused by the SOW influence in the zonal components of the general circulation of the atmosphere and amplitudes of planetary waves.

This paper presents the results of the numerical simulation of possible changes in the meridional and vertical velocities in the middle atmosphere, as well as in vertical ozone fluxes in the strato-mesosphere, caused by accounting for SOW effects in the numerical model of the general circulation of the middle and upper atmosphere.

2. OROGRAPHY PARAMETERIZATION AND NUMERICAL MODEL

Ground atmospheric flow around the relief of the Earth's surface is an important source of stationary mesoscale waves in the atmosphere. In this work, we use the parameterization described by Gavrilov and Koval (2013) for the dynamic and thermal effects of SOWs in the atmosphere. The total vertical wave

energy flow and the vertical profile of the fluctuation amplitude of the horizontal velocity are calculated in this parameterization using polarization relations obtained by the authors for stationary orographic waves taking the atmosphere rotation into account. According to these relations, the wave acceleration and total wave heat influx are calculated. They can be used for the parameterization of the dynamic and thermal effects of stationary gravity waves in atmospheric dynamic models (see (Gavrilov and Koval, 2013)). The mesoscale orography is parameterized in this work using a modification of the method developed by Scinocca and McFarlane (2000). This method uses the concept of "subgrid" orography, which includes variations in the height of the Earth's surface with horizontal scales that are less than the spacing of the horizontal grid of the numerical model; they are determined by applying low- and high-frequency numerical filters to the real distribution of heights of the Earth's surface. In this work, the described parameterization is practically implemented using the ETOPO2 database for height of the Earth's surface with a step of 2 min along the latitude and longitude.

When studying the SOW influence on the atmosphere dynamics and ozone fluxes, the aforementioned parameterization was incorporated into the numerical model of circulation of the middle and upper atmosphere (MCMUA) (Pogorel'tsev, 2007; Pogoreltsev et al., 2007), developed based on the model of Cologne University, Germany (Jacobs et al., 1986). The model is based on solving a standard system of primitive equations in spherical coordinate system (Jacobs et al., 1986). It involves parameterizations of atmosphere heating in the UV and visible regions of the spectrum from 125 to 700 nm, as well as coolings in the 8, 9.6, 14, and 15 μm bands of IR radiation. For heights of the lower thermosphere, additional dynamic heat sources are taken into account. In the thermosphere, ion deceleration, molecular viscosity, and heat conduction, as well as turbulent diffusion at heights of the mesosphere and lower thermosphere, are involved. The calculations are performed for heights from 0 to 150 km; however, weather changes in the troposphere are in fact not modeled. The Marchuk-Strang splitting scheme (Marchuk, 1967; Strang, 1968) was applied. Integration with respect to time is performed using a scheme proposed by Matsuno (1966). The solution stability is maintained by a Fourier filter, which restricts the zonal resolution to ~500 km. The spacings of the horizontal grid of the model are 5.6° in longitude and 5° in latitude in the range from 87.5° S to 87.5° N. The vertical grid has a constant spacing in the coordinate $z = H\ln(p_0/p)$, where p_0 is the surface pressure and $H = 7$ km. Different versions of the model have 48 or 64 vertical nodes with a spacing $\Delta z \sim 2.7$ km. In the presented calculations, a model version with 48 vertical levels was used. The time integration step is 450 s.

The global ozone distribution in the atmosphere was taken into account in the numerical model by a semiempirical model (Fortuin and Langematz, 1995), which yields zone-averaged monthly mean values of the ratio of the ozone mixture at 34 height levels corresponding to the atmospheric pressure from 1000 to 0.003 hPa. The zone-averaged vertical ozone flux F_{O3i} at grid node, with the number i is calculated by the formula

$$F_{O3i} = N_{O3i} w_i, \quad N_{O3i} = 10^{-6} \rho_i X_{O3i} N_A / \rho_0, \qquad (1)$$

where w_i is the monthly mean vertical velocity averaged with respect to longitude, ρ_0 is the ground density of the atmosphere at normal conditions, X_{O3i} is the zone-averaged ozone mixing ratio in millions^{-1}, and N_A is the Avogadro number.

3. RESULTS OF CALCULATIONS

To study the influence of orographic waves generated by the relief of the Earth's surface and propagating upward on the meridional and vertical velocity components created by the general circulation of the atmosphere, calculations were performed using the described MCMUA model with included parameterization of the dynamic and thermal SOW effects (see Sect. 2). The calculations were performed for conditions corresponding to January and July. For every set of the initial data, fields for the meridional and vertical components of wind velocity were calculated with and without inclusion of SOW effects. The differences of values between these calculations demonstrate velocity increments (VIs) caused by the dynamic and thermal SOW effects in the middle atmosphere. Positive or negative values of the VI indicate an increase or decrease in the corresponding velocity component due to SOW effects.

Figure 1a presents the height-latitude distribution of the calculated vertical velocity for January. Lines with arrows correspond to schematic zonal averaged streamlines calculated in the following way: values of the vertical velocity w were multiplied for the sake of illustration by a factor of 3×10^3. In Fig. 1a, below 60–70 km, the main cell of the meridional circulation is seen with an air upward flow near the equator and in low latitudes of the summer (Southern) hemisphere and its downward flow at latitudes of 20°–50° of the winter (Northern) hemisphere. In addition, in Fig. 1a, below 60 km, one can observe weaker cells with air ascend at latitudes of 50°–70° of both the hemispheres and air descend to the South and North from the rise zone. At heights exceeding 60–70 km in Fig. 1a, there prevails a meridional circulation cell with an ascend at middle and high latitudes of the summer hemisphere and a descend in middle and high latitudes of the winter hemisphere.

Figure 1b shows a vertical velocity increment (VVI) caused by the SOW influence. One can see regions of

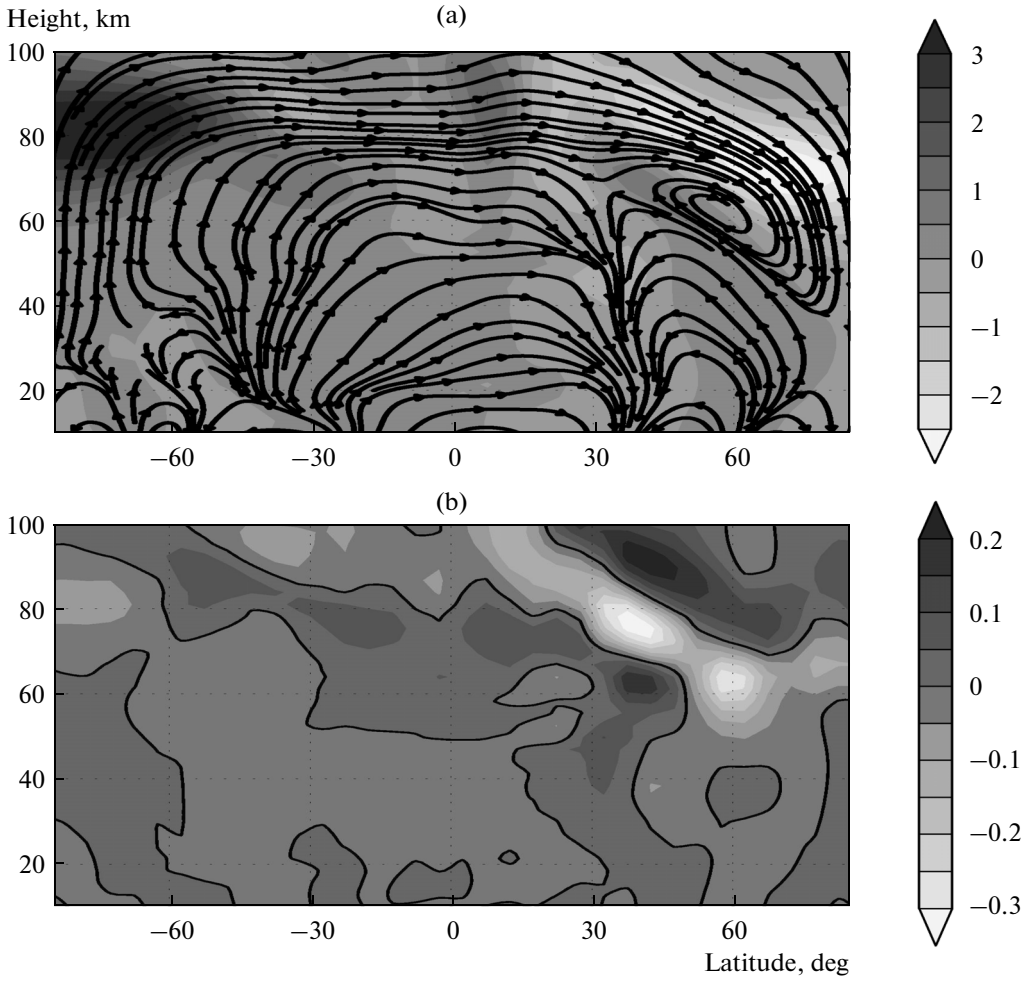

Fig. 1. January height-latitude distributions of the (a) vertical velocity (cm/s) and (b) its increments due to the SOW influence. The arrows show the direction of schematic streamlines.

positive and negative VVIs corresponding to an increase or decrease in the vertical velocity with inclusion of the SOW effects. In many cases in Fig. 1b, VVI signs are opposite to those of the vertical velocity in Fig. 1a, i.e., SOW action leads to an attenuation of zonal average vertical fluxes. Peak VVIs in Fig. 1b can reach ±25–30% of peak values of the vertical velocity at corresponding heights in Fig. 1a.

Figure 2a is similar to Fig. 1a but for July. At heights less than 60–70 km, one can see, by analogy with January, a circulation cell with an air ascend near the equator and in low latitudes of the summer (now, Northern) hemisphere and an air sink in middle latitudes of the winter (Southern) hemisphere. In addition, below 40–50 km in Fig. 2a, there is seen an air ascend at latitudes of 60°–70° of both hemispheres. At heights exceeding 60–70 km, ascending flows in middle and high latitudes of the summer (now, Northern) hemisphere and an air mass sink in middle and high latitudes of the winter (Sothern) hemisphere prevail. At heights of 80–100 km, perturbations of this main flow can appear with the formation of smaller local circulation cells (see Fig. 2a). Increments of the vertical velocity in Fig. 2b can reach ±10% of peak values of the vertical velocity in Fig. 2a.

Figures 3a and 4a show latitude-longitude vertical velocity distributions at a height of 25 km for January and July, respectively. One can see periodic (with respect to longitude) air ascend and descend regions of the planetary wave type; the wave amplitude is larger in winter (Northern in January and Southern in July) hemispheres.

Figures 3b and 4b represent latitude-longitude VVI distributions affected by SOWs. One can find periodic (with respect to longitude) variations in VVI signs, which are often the opposites of signs of periodic structures of the vertical velocity in Figs. 3a and 4a. It is most noticeable when comparing Figs. 3a and 3b for January. Values of local extreme VVIs in Figs. 3b and 4b can reach ±30–50% of extreme values of w in Figs. 3a and 4a. An interesting feature of Figs. 3b and 4b is the presence of VVI maximums over regions of higher

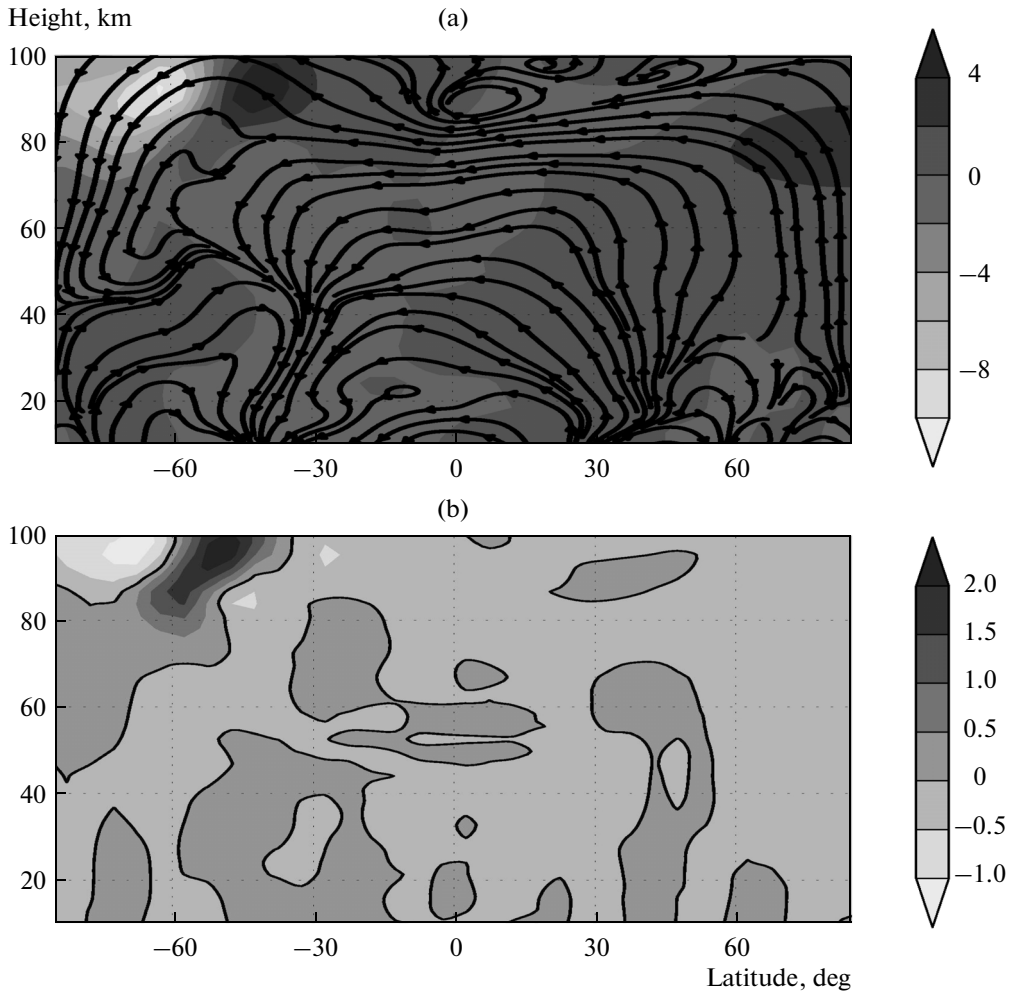

Fig. 2. Same as in Fig. 1 but for July.

mountain systems (the Himalayas and Rocky Mountains in the Northern hemisphere and the Andes in the Southern hemisphere). These maximums are observed both in January (Fig. 3b) and in July (Fig. 4b). They demonstrate that SOW action can lead to the formation of quasi-stationary large-scale ascending flows over mountain systems.

According to the formula (1), vertical displacements of air particles in the process of the general circulation of the atmosphere create vertical fluxes of ozone and other gas species, which play an important part in the climate formation. The ozone distribution used in the MCMUA numerical model was verified (Suvorova and Pogorel'tsev, 2011) by comparing it with the empirical model by Randel and Wu (2005). A sufficiently good correspondence between the zonal average ozone concentration distributions used in our version of the MCMUA model and the empirical model was obtained.

Figures 5a and 6a present the height-latitude structures of the vertical ozone flux component calculated by formula (1) for January and July, respectively. Below 60–70 km, one can see zones of positive values of ozone fluxes in near-equatorial and low latitudes of summer hemispheres, as well as those of negative F_{O3} in middle latitudes of both hemispheres, which corresponds to the distributions of the vertical velocities in Figs. 1a and 2a, as well as to the existing knowledge about ozone transport by the general circulation of the atmosphere (Holton et al., 1995; Holton, 2002). In addition, below 50–60 km in Figs. 5a and 6a, one can see regions of ascending ozone fluxes (positive F_{O3}) at latitudes of 45°–80° in both the hemispheres. In winter hemispheres, these ascending ozone fluxes are stronger and propagate to larger heights than in summer hemispheres. This ozone ascend is accompanied by regions of descending (negative) ozone fluxes located to the North and to the South (see Figs. 5a and 6a), which leads to the appearance of additional cells of ozone circulation in middle latitudes by analogy with cells of the meridional circulation in Figs. 1a and 2a. At heights exceeding 60–70 km in Figs. 5a and 6a, ascending ozone fluxes in summer hemispheres and

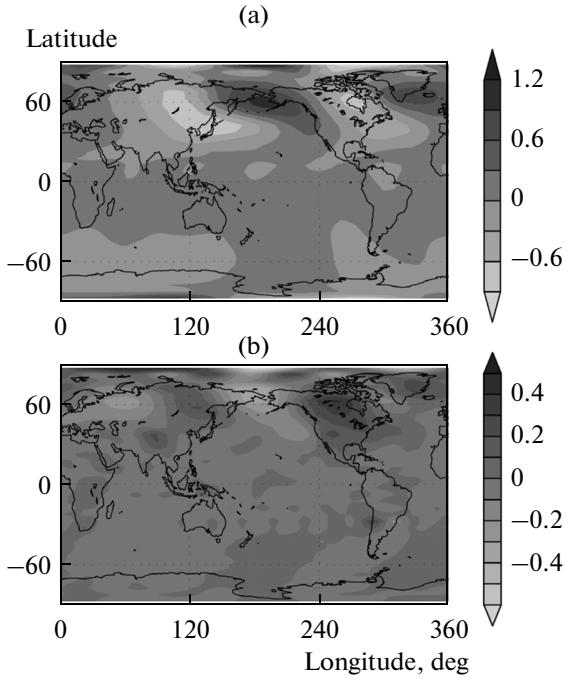

Fig. 3. January latitude-longitude distributions of the (a) vertical velocity (cm/s) and (b) its increments due to the SOW influence at a height of 25 km.

downward fluxes in winter hemispheres prevail. Local perturbations of the meridional circulation at heights of 80–100 km (Fig. 2a) can lead to local changes in the vertical transfer in regions of these perturbations (see Fig. 6a).

Increments of zonal average vertical ozone fluxes (OFIs) appearing due to the inclusion of orographic wave parameterization into the model are presented in Figs. 5b and 6b for January and July, respectively. One can see regions of positive and negative OFI values, which correspond to an increase or decrease in vertical ozone fluxes. Absolute values of OFI extreme values in Fig. 2b are larger in the Northern (winter) hemisphere and can exceed ±20% of extreme values of ozone fluxes in Figs. 5a and 5b at heights of 10–30 km. This is explained by better conditions of SOW propagation and by the stronger influence of waves on the general circulation of the atmosphere in winter hemispheres as compared to summer ones (Gavrilov and Koval, 2012; Gavrilov et al., 2012). It means that the SOW influence can lead to significant changes in ozone circulation in the region of the ozone layer maximum, which can have a significant effect on the exchange of optically active gas species between the troposphere and stratosphere.

Similar calculations performed for equinox periods demonstrated that regions of maximum and minimum OFI values are more uniformly distributed in the Northern and Southern hemispheres and also correspond to regions of preferable SOW propagation into the middle atmosphere. In April, regions of preferable SOW propagation and maximum OFIs are located in high latitudes of the Southern hemisphere and in middle latitudes of the Northern hemisphere. In October, preferable SOW propagation exists in latitudes of main

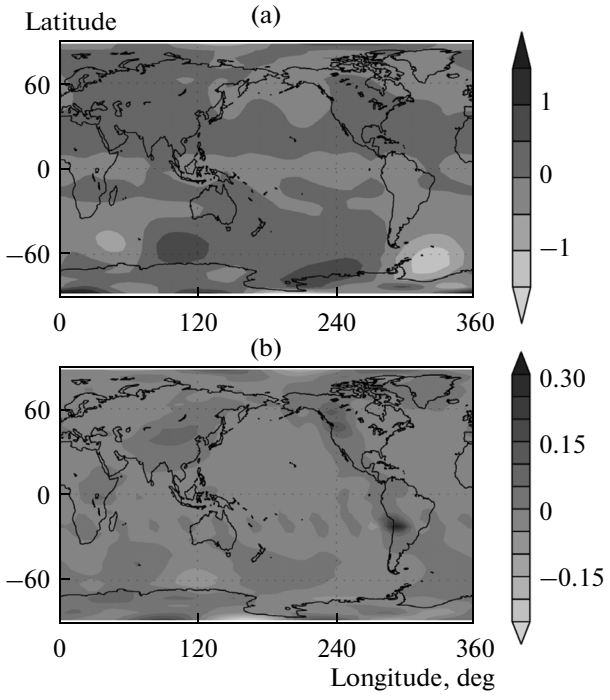

Fig. 4. Same as in Fig. 3 but for July.

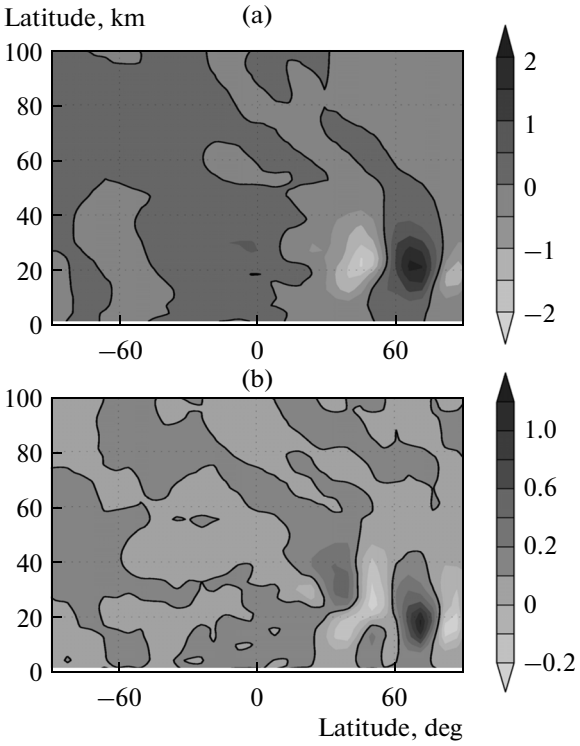

Fig. 5. Height-latitude distributions of (a) zone-averaged values of the vertical ozone flux F_{O3} in 10^{14} m^{-2} s^{-1} and (b) increments of ozone fluxes due to the SOW influence for January.

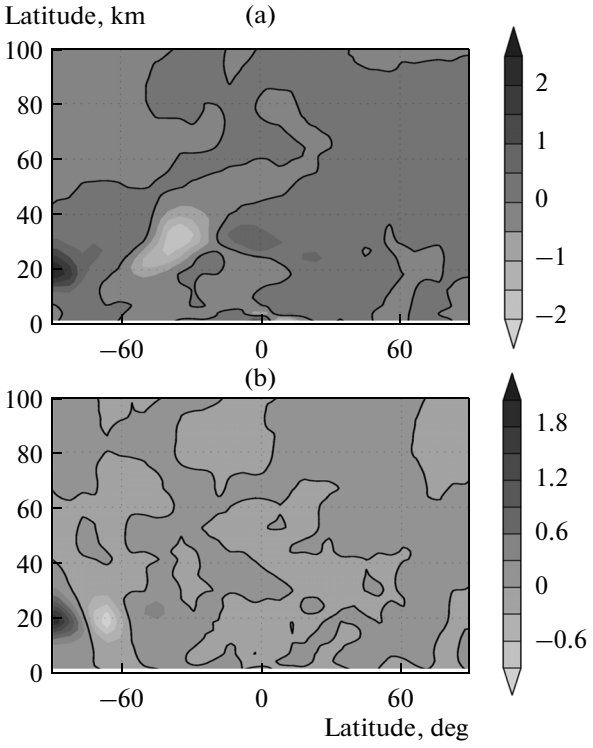

Fig. 6. Same as in Fig. 5 but for July.

mountain systems in the Northern hemisphere and toward the largest OFIs over these regions.

4. CONCLUSIONS

The developed parameterization of the dynamic and thermal effects of SOWs generated by the relief of the Earth's surface is included into the numerical model of the general circulation of the middle and upper atmosphere. Possible changes in the meridional circulation of the atmosphere under changes in the conditions of SOW generation and propagation in different seasons are modeled. It is shown that taking into account the dynamic and thermal SOW effects in the numerical model leads to changes in the vertical velocity and ozone fluxes connected with it by up to 20–30% at the heights of the ozone layer maximum. Thus, numerical simulation shows that inclusion of orographic waves can lead to significant changes in meridional circulation and ozone fluxes in the upper troposphere and stratosphere. This must be taken into account when modeling the atmospheric global circulation and variations in the chemical composition of the atmosphere. The involved numerical model does not describe the influence of the dynamics on ozone distribution. The aforementioned ozone flux changes are therefore connected only with vertical velocity changes due to the SOW influence. It seems advisable to carry out a similar investigation of the SOW influ-

ence on ozone fluxes using models taking into account the influence of the circulation on the atmosphere composition.

ACKNOWLEDGMENTS

This work was supported by the Russian Foundation for Basic Research and Ministry of Education and Science of the Russian Federation in the scope of the Scientific and Scientific-Pedagogical Personnel of Innovative Russia federal target program for 2009–2013 (state contract no. P107).

REFERENCES

Danielsen, E.F. and Mohnen, J., Project dustorm report: ozone transport, in situ measurements and meteorological analyses of tropopause folding, *J. Geophys. Res.*, 1977, vol. 82, pp. 5867–5877.

Fishman, J. and Crutzen, P.J., The origin of ozone in the troposphere, *Nature*, 1978, vol. 274, pp. 855–857.

Fortuin, J.P.F. and Langematz, U., An update on the global ozone climatology and on concurrent ozone and temperature trends, *Atmospheric Sensing and Modeling, Proc. SPIE,* 1995, vol. 2311, pp. 207–216.

Gavrilov, N.M. and Koval, A.V., Parameterization of mesoscale stationary orographic wave forcing for use in numerical models of atmospheric dynamics, *Izv. Akad. Nauk, Fiz. Atmos. Okeana,* 2013, vol. 49, pp. 244–251.

Gavrilov, N.M., Koval, A.V., Pogoreltsev, A.I., and Savenkova, E.N., Numerical simulation of the response of general circulation of the middle atmosphere to spatial inhomogeneities of orographic waves, *Izv. Akad. Nauk, Fiz. Atmos. Okeana*, 2013a, vol. 49, pp. 367–374.

Gavrilov, N.M., Koval, A.V., Pogoreltsev, A.I., and Savenkova, E.N., Numerical modeling of inhomogeneous orographic wave influence on planetary waves in the middle atmosphere, *Adv. Space Res.*, 2013b, vol. 51, pp. 2145–2154.

Holton, J.R., Stratosphere–Troposphere Exchange, in *Encyclopedia of Atmospheric Sciences*, Holton, J.R, Pyle, J., and Curry, J.A., Eds., New York: Academic, vol. 5, 2003, pp. 2137–2143.

Holton, J.R., Haynes, P.H., McIntire, M.E., Douglas, A.R., Rood, R.B., and Pfister, L., Stratosphere–troposphere exchange, *Rev. Geophys.*, 1995, vol. 33, pp. 403–439.

Jakobs, H.J., Bischof, M., Ebel, A., and Speth, P., Simulation of gravity wave effects under solstice conditions using a 3-d circulation model of the middle atmosphere, *J. Atmos. Terr. Phys.*, 1986, vol. 48, pp. 1203–1223.

Marchuk, G.I., *Chislennye metody v prognoze pogody* (Numerical Methods in the Weather Forecast), Leningrad: Gidrometeoizdat, 1967.

Matsuno, T., Numerical integration of the primitive equations by a simulated backward difference method, *J. Meteorol. Soc. Jpn.*, 1966, vol. 44, pp. 76–84.

Pogoreltsev, A.I., Generation of normal atmospheric modes by stratospheric vacillations, *Izv. Akad. Nauk, Fiz. Atmos. Okeana*, 2007, vol. 43, pp. 423–435.

Pogoreltsev, A.I., Vlasov, A.A., Froehlich, K., and Jacobi, Ch., Planetary waves in coupling the lower and upper atmosphere, *J. Atmos. Sol.-Terr. Phys.*, 2007, vol. 69, pp. 2083–2101.

Randel, W.J. and Wu, F., A stratospheric ozone profile data set for 1979–2005: variability, trends, and comparisons with column ozone data, *J. Geophys. Res.*, 2007, vol. 112, p. D06313.

Scinocca, J.F. and McFarlane, N.A., The parameterization of drag induced by stratified flow over anisotropic orography, *Q. J. Roy. Meteor. Soc.*, 2000, vol. 126, pp. 2353–2393.

Strang, G., On the construction and comparison of difference schemes, *SIAM J. Numer. Anal.*, 1968, vol. 5, pp. 516–517.

Suvorova, E.V. and Pogoreltsev, A.I., Modeling of nonmigrating tides in the middle atmosphere, *Geomagn. Aeron.*, 2011, vol. 51, pp. 105–115.

Translated by A. Nikol'skii